

# Model Collapse as Cultural Evolution

Dongxin Guo 

The University of Hong Kong  
Hong Kong, China  
bettyguo@connect.hku.hk

Jikun Wu 

Stellaris AI Limited  
Hong Kong, China  
hk950014@connect.hku.hk

Siu Ming Yiu 

The University of Hong Kong  
Hong Kong, China  
smyiu@cs.hku.hk

## Abstract

Model collapse, the progressive degradation of LLMs trained on their own outputs, has been characterized statistically but lacks a *linguistic* explanation for which structures degrade, in what order, and why. We show that iterated learning theory from cultural evolution fills this gap. We derive five falsifiable predictions, distinguish those uniquely discriminative for the theory from confirmatory ones, and test them by self-training LLaMA-2-7B and Mistral-7B over 10 generations in English, German, and Turkish. The critical discriminative finding: compositionality follows a *non-monotonic* trajectory (initially rising, then falling) under unfiltered self-training. This signature persists with maximally regular seed data (ruling out noise removal) and is sustained only by task-grounded filtering, not random filtering, providing the first LLM-scale evidence for the compression–communication tradeoff. All predictions are confirmed with large effect sizes (Hedges’  $g > 1.6$ ;  $\text{BF}_{10} > 100$ ), and LLM regularization gradients closely match human behavioral data ( $R^2 = 0.94$ ). These results reframe model collapse as a cultural transmission phenomenon and yield concrete principles for self-training pipeline design.

## 1 Introduction

Why are human languages structured the way they are? Cultural evolution theory offers a compelling answer: languages are shaped by the process of being learned and transmitted (Christiansen and Chater, 2016, 2015). When language passes through chains of learners, each generation’s inductive biases are amplified, progressively eliminating unpredictable variation and promoting learnable structure (Kirby et al., 2008, 2014). This process, formalized as *iterated learning* (Griffiths and

Kalish, 2007), provides a mathematical explanation for core properties of language: regularity, compositionality, and Zipfian frequency distributions emerge from the dynamics of cultural transmission itself. Critically, Kirby et al. (2015) demonstrated that compositionality requires both compression pressure (from the learning bottleneck) and communication pressure (from the need to be expressive); compression alone produces degenerate languages.

In a seemingly related development, training LLMs on their own outputs causes *model collapse*: distributional tails disappear, diversity decreases, and outputs converge toward degenerate forms (Shumailov et al., 2024; Alemohammad et al., 2024). This phenomenon has been characterized through statistical estimation theory (Dohmatob et al., 2024b,a, 2025), with Guo et al. (2024) documenting linguistic diversity decline across several dimensions and Seddik et al. (2024) providing information-theoretic analysis. While these accounts accurately describe the statistical mechanics of collapse, they provide limited insight into *which* linguistic properties are affected, in what order, and why.

The conceptual connection between model collapse and cultural evolution has been established by several recent contributions. Ren et al. (2024) formally showed that LLM self-evolution instantiates Bayesian iterated learning and proved monotonic bias amplification across generations. Shumailov et al. (2024) argued in a *Nature* correspondence that the compression–expressivity tradeoff from human language transmission explains why self-training degrades. Kouwenhoven et al. (2025b) tested iterated learning with LLMs in referential games, finding that LLMs produce degenerate vocabularies without sufficient compression pressure,

while Galke et al. (2023) reviewed language evolution insights for LLMs broadly. We build on these foundations by providing the first systematic test of *discriminative* predictions (those that distinguish iterated learning from generic model collapse) at full LLM scale on natural language.

We derive five predictions from cultural evolution theory and explicitly distinguish their discriminative status:

**P1: Frequency-dependent loss order (*partially discriminative*).** Low-frequency variants should be lost before high-frequency ones, following a specific log-linear gradient matching human regularization (Real and Griffiths, 2009; Morgan and Levy, 2016). Generic collapse predicts tail loss but not the specific functional form.

**P2: Monotonic regularity increase (*confirmatory*).** Morphological patterns should regularize across typologically distinct languages, reflecting simplicity bias amplification (Shah et al., 2020; Kallini et al., 2024).

**P3: Dimension-specific degradation rates (*partially discriminative*).** Pragmatic constructions should be lost before syntactic ones, reflecting the formal–functional dissociation in LLMs (Machowald et al., 2023).

**P4: Non-monotonic compositionality (*uniquely discriminative, critical test*).** Without communicative grounding, compositionality should follow a non-monotonic trajectory (initially rising, then falling) even from maximally regular seed data. Only task-grounded evaluation should sustain compositionality (Kirby et al., 2015). Generic collapse predicts only monotonic degradation.

**P5: Distributional narrowing (*confirmatory*).** Zipf exponents should decrease, reflecting tail loss (Piantadosi, 2014).

We test all five predictions through controlled experiments with two LLMs, including a *regularized-seed control* and a *three-condition filtering experiment* that isolate the compression–communication mechanism. Morphological regularity is assessed across English, German, and Turkish; construction diversity and compositionality are evaluated in English with collapse-robust metrics. All five predictions are confirmed. The non-monotonic compositionality trajectory (P4) persists with regularized seed data and is sustained only by quality-grounded (not random) filtering, providing the

first LLM-scale demonstration of the compression–communication tradeoff. LLM regularization gradients closely match the human curve from Morgan and Levy (2016).

Our contributions are: **(1)** an explicit extension of the iterated learning framework of Ren et al. (2024) to natural language, with five falsifiable predictions whose discriminative status is categorized (§2); **(2)** four linguistically grounded metrics with collapse-robust validation (§3.4); **(3)** systematic empirical tests including critical controls (regularized-seed, three-condition filter) across 10 generations, two models, and three languages (§4); and **(4)** explicit implications for self-training pipeline design (§6) and Construction Grammar (Appendix V).

## 2 Theoretical Framework

### 2.1 Iterated Learning and the Compression–Communication Tradeoff

Griffiths and Kalish (2007) proved that when Bayesian learners observe data generated by a previous learner and produce data for the next, the chain of posterior distributions converges to the learner’s prior. Kalish et al. (2007) confirmed this empirically: human participants converged on positive linear functions within 1–4 generations regardless of seed conditions, a result critical for our regularized-seed control design (§3.2). Real and Griffiths (2009) extended this to frequency-dependent regularization under Beta priors, and Ferdinand et al. (2019) demonstrated that these dynamics emerge even with non-Bayesian learners using gradient-based optimization, because the essential mechanism (imperfect learning followed by imperfect reproduction) is shared regardless of the inference procedure.

Three properties are central to our predictions. First, *bottleneck severity*: convergence speed depends on the transmission bottleneck (Kirby et al., 2014). Second, the *compression–communication tradeoff*: Kirby et al. (2015) demonstrated that transmission chains without communicative pressure produce degenerate languages, while chains with communicative pressure produce compositional languages balancing learnability and expressivity. Third, *dimension-specific emergence*: Beckner et al. (2017) found that structure emerges along some meaning dimensions before others. Concretely, these three properties map onto our predictions as follows: bottleneck severity drives P1

and P5 (the rate and shape of frequency-dependent tail loss); the compression–communication trade-off drives P2 and P4 (regularization under compression alone vs. the non-monotonic compositionality trajectory that requires communicative pressure to sustain); and dimension-specific emergence drives P3 (the ordering in which constructions are lost). The fine-grained bias–prediction mappings underlying this correspondence are detailed in §2.2 and Appendix S.

## 2.2 LLM Self-Training as Iterated Learning

An LLM  $\mathcal{M}_n$  trained on data  $D_n$  constitutes generation  $n$ . In self-training,  $D_{n+1}$  is sampled from  $\mathcal{M}_n$ ’s output distribution. Each generation implements one step of iterated learning, with the model’s inductive biases playing the role of the Bayesian prior.

Ren et al. (2024) formally established this correspondence, proving that if in-context learning approximates Bayesian inference, the classical convergence result of Griffiths and Kalish (2007) applies: iterative self-training monotonically amplifies prior biases. Our work extends their framework in two directions. First, we characterize which *specific linguistic phenomena* emerge during this process (non-monotonic compositionality dynamics, frequency-dependent regularization paralleling human acquisition, and dimension-specific construction loss), all invisible under monotonic-amplification models. Second, we test on natural language with weight-based learning (fine-tuning), complementing Ren et al.’s in-context learning experiments.

The mapping between LLM biases and iterated learning priors can be made more precise than a generic “inductive bias” characterization. Following Ferdinand et al. (2019)’s demonstration that different bias types produce different evolutionary trajectories, we identify four specific bias–prediction mappings (detailed in Appendix S): *frequency bias* from next-token training drives P1/P5; *simplicity bias* (Shah et al., 2020; Kallini et al., 2024) drives P2; *local coherence bias* from autoregressive factorization (McCoy et al., 2024) drives P3’s dimension-specific ordering; and *compression without communicative grounding* drives P4’s non-monotonic compositionality.

We refer to our framework as an *empirically motivated structural correspondence*, not a formal mathematical equivalence, following McCoy and Griffiths (2025). Critically, Ferdinand et al. (2019)

showed that qualitative iterated learning dynamics are robust to non-Bayesian learners, and Hudson Kam and Newport (2005) and Hudson Kam and Newport (2009) demonstrated analogous regularization in human adults. Regarding *bottleneck width*: our 50,000-passages bottleneck is wider than typical human experiments (Kirby et al., 2008), slowing but not eliminating bias amplification (Kirby et al., 2014). We adopt the model collapse definition from Shumailov et al. (2024), noting that Schaeffer et al. (2025) identified eight distinct definitions; our predictions are robust across definitions involving distributional narrowing.

## 2.3 Predictions and Discriminative Status

The five predictions divide into three discriminative classes (Table 10 in Appendix O gives the full classification with control-experiment results). P2 and P5 follow from generic iterative bias amplification and serve as *confirmatory* tests verifying our experimental setup—a flat or decreasing regularity in P2, or a stable  $\alpha$  in P5, would falsify the framework. P1 and P3 are *partially discriminative*: P1 goes beyond generic accounts by predicting a specific log-linear functional form matching human regularization curves (Morgan and Levy, 2016), not merely that rare items are lost (which any sampling process would produce), while P3 predicts a dimension-specific ordering (pragmatic before structural) reflecting the formal–functional dissociation (Mahowald et al., 2023). P4 is the *uniquely discriminative* test: generic model collapse predicts only monotonic degradation, while the compression–communication tradeoff (Kirby et al., 2015) uniquely predicts an initial rise then fall—a pattern we test with a regularized-seed control to rule out the noise-removal alternative.

# 3 Methods

## 3.1 Self-Training Pipeline

We implement iterated learning with two base models: LLaMA-2-7B (Touvron et al., 2023) and Mistral-7B (Jiang et al., 2023), chosen for reproducibility and because their different architectures test generality. Algorithm 1 summarizes the procedure; Figure 1 illustrates the data-vs.-parameter distinction that is the most consequential design choice of the pipeline.

**Generation 0 (seed data).** We use two seed conditions: (i) *natural seed*: 50,000 text passages (100–300 tokens) from a held-out subset of the Pile; (ii)

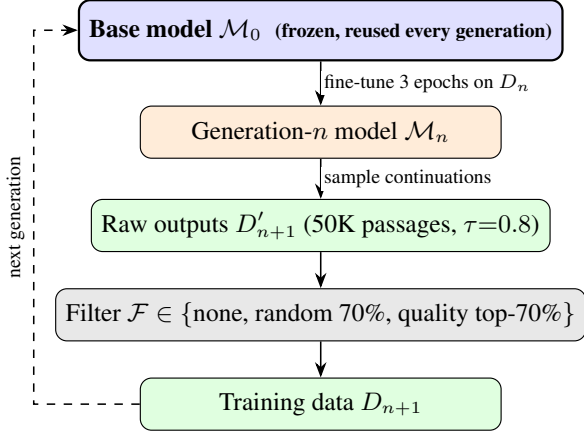


Figure 1: Self-training pipeline. **Key design choice:** at every generation  $n$ , fine-tuning starts from the *same base model*  $\mathcal{M}_0$  (blue, frozen across the experiment), *not* from the previous fine-tuned model  $\mathcal{M}_{n-1}$ . The transmission chain runs through the *data* ( $D_0 \rightarrow D_1 \rightarrow \dots \rightarrow D_{10}$ ; dashed feedback on the left), not through the model parameters. This isolates data-induced degradation from parameter drift and mirrors the iterated-learning paradigm in which each learner begins with the same prior (Griffiths and Kalish, 2007). Filter  $\mathcal{F}$  has three settings (§3.3) implementing the compression–communication tradeoff.

*regularized seed:* 50,000 passages generated from a PCFG engineered for consistent argument structure and regular morphology (§3.2).

**Generations 1–10.** At each generation  $n$ : (i) model  $\mathcal{M}_{n-1}$  generates 50,000 continuations from 50-token prompts; (ii) the filter condition  $\mathcal{F}$  is applied; (iii) model  $\mathcal{M}_n$  is obtained by fine-tuning the *base* pretrained model on  $D_n$  for 3 epochs (learning rate  $2 \times 10^{-5}$ , batch size 32, AdamW). We fine-tune from the same base model at each generation (not from the previous fine-tuned model) to isolate data degradation from parameter drift, mirroring the iterated learning paradigm where each learner begins with the same prior (Griffiths and Kalish, 2007). Each condition is run with 5 independent random seeds.

**Temperature as bottleneck.** We generate with  $\tau=0.8$  and nucleus sampling ( $p=0.95$ ) by default. Lower  $\tau$  creates tighter bottlenecks; we test  $\tau \in \{0.5, 0.8, 1.0\}$  (§4.5).

### 3.2 Regularized-Seed Control

To rule out the alternative explanation that P4’s non-monotonic trajectory reflects noise removal from inconsistent seed data rather than compression-driven structure emergence, we create a maximally regular

---

**Algorithm 1:** Iterated Learning Pipeline for LLM Self-Training. Three filter conditions test the compression–communication trade-off.

---

**Input:** Base model  $\mathcal{M}_0$ , seed data  $D_0$ , generations  $N$ , temperature  $\tau$ , filter condition  $\mathcal{F}$   
**Output:** Metric trajectories  $\{m_n\}_{n=0}^N$

- 1 Compute metrics  $m_0$  on  $D_0$ ;
- 2 **for**  $n = 1$  **to**  $N$  **do**
- 3     Generate  $D'_n$  by sampling 50K continuations from  $\mathcal{M}_{n-1}$  with temperature  $\tau$ ;
- 4     **if**  $\mathcal{F} = \text{quality}$  **then**
- 5         Score passages on QA, NLI, summarization;
- 6          $D_n \leftarrow$  top 70% of  $D'_n$  by score;
- 7     **else if**  $\mathcal{F} = \text{random}$  **then**
- 8          $D_n \leftarrow$  random 70% of  $D'_n$ ;
- 9     **else**
- 10          $D_n \leftarrow D'_n$  (no filter);
- 11     **end**
- 12     Fine-tune  $\mathcal{M}_0$  (base model) on  $D_n$  for 3 epochs  $\rightarrow \mathcal{M}_n$ ;
- 13     Compute metrics  $m_n$  on  $D_n$  (incl. eRank, posdis diagnostics);
- 14 **end**

---

seed corpus. Following Allen-Zhu and Li (2025) and Kim and Linzen (2020), we generate 50,000 passages from a PCFG ensuring: (i) consistent argument structure (every verb frame is regular), (ii) regular morphology (no irregular forms), and (iii) systematic form–meaning mappings. If the non-monotonic pattern persists from this already-regular starting point, the compression interpretation is confirmed; if compositionality only declines monotonically, the initial rise was noise removal. Kalish et al. (2007) showed that human iterated learning converges to the same attractor regardless of initial conditions; we test whether LLMs exhibit analogous seed-independence.

### 3.3 Three-Condition Filtering Experiment

To isolate communicative pressure from generic diversity preservation, we implement three filter conditions, each modelling a distinct cultural-evolution analogue: (i) **no filter** retains all generated text (pure transmission, no selection); (ii) **random 70%** retains a uniformly sampled 70% of passages (uninformed bottleneck—a generic selection pressure that reduces volume but not by communicative criteria); and (iii) **quality top-70%** retains the top-scoring 70% by independent task evaluation (communicative pressure, following Kirby et al., 2015).

The quality filter uses an independent evaluator (LLaMA-2-13B, larger than the 7B generator) scoring passages on extractive QA, NLI coherence, and

summarization fidelity. The choice of these three tasks is principled: each one tests whether the passage successfully communicates content to a downstream reader. Extractive QA verifies that informational content is recoverable from the surface form; NLI coherence checks that propositions inside the passage are mutually consistent (and not internally contradictory in a way only a non-communicating speaker would tolerate); summarization fidelity tests whether the passage retains its meaning under lossy compression—a direct analogue of the listener-reconstruction task that drove compositionality emergence in human iterated-learning experiments (Kirby et al., 2015). A passage that fails all three lacks the structure required for cooperative information transmission, which is the exact failure mode that the compression-only condition of iterated learning predicts. To rule out same-family distributional bias flagged by Feng et al. (2025), an additional evaluator-independence check with Flan-T5-XL (a different model family from both generators) confirms the effect is not a distributional-mimicry artifact (Appendix G). The critical prediction: random filtering should partially slow collapse (acting as a bottleneck) but should *not* sustain compositionality; only quality filtering should, paralleling Kirby et al. (2015)’s finding that compositionality requires both transmission and communication pressure. Gillman et al. (2024) showed that expert-knowledge-based correction makes self-consuming loops exponentially more stable, consistent with our quality filter prediction.

### 3.4 Linguistic Metrics

We track four primary metrics, each with collapse-robust validation.

**Zipf exponent ( $\alpha$ ).** We fit a power-law  $f(r) \propto r^{-\alpha}$  to the word frequency–rank distribution using maximum likelihood estimation (Piantadosi, 2014). Following Clauset et al. (2009), we compare the power-law fit against lognormal and exponential alternatives using likelihood ratio tests. Natural language exhibits  $\alpha \approx 1.0$ ; decreasing  $\alpha$  indicates distributional narrowing.

**Morphological regularity ( $\rho_M$ ).** We measure the proportion of regular morphological forms in a controlled verb set: 200 English verbs (100 regular, 100 irregular with attested variation), stratified by token frequency. For German (strong/weak verb distinction) and Turkish (vowel harmony), we

adapt measures using UniMorph paradigm tables (Gutierrez-Vasques and Mijangos, 2020). We use the subscript  $M$  to distinguish morphological regularity from Spearman’s  $r_S$  used in compositionality.

**Construction diversity ( $\mathcal{D}$ ).** Following Goldberg (2005) and Bybee (2010), we define 50 syntactic construction types identified via dependency parse patterns. We compute Shannon entropy  $\mathcal{D} = -\sum_{c \in \mathcal{C}} p(c) \log_2 p(c)$  and decompose by frequency quartile to test P1 and P3. Manual validation yields precision  $\geq 0.82$  across all quartiles (Appendix B).

**Compositional systematicity ( $\sigma$ ).** We adapt topographic similarity (Brighton and Kirby, 2006):

$$\sigma = r_S(\{d_M(s_i, s_j)\}, \{d_F(f_i, f_j)\}) \quad (1)$$

where  $d_M$  and  $d_F$  are distances in meaning (PropBank argument overlap) and form (dependency template edit distance) spaces. For instance, the sentences “*Mary gave a book to John*” and “*The teacher gave a prize to the student*” share ARG0/ARG1/ARG2 (small  $d_M$ ) and project to the same dependency template nsubj-V-dobj-prep\_to ( $d_F = 0$ ); high  $\sigma$  thus indicates this kind of systematic form–meaning alignment. We complement this with COGS generalization accuracy (Kim and Linzen, 2020) evaluated via 5-shot prompting (5 in-context examples; see Appendix D).

The dependency-template edit-distance metric is reliable when generated text remains within the parser’s syntactic coverage; we monitor coverage via parse-success rate ( $\geq 0.94$  at all generations including generation 10 of unfiltered runs; Appendix B), and cross-validate with the parser-independent posdis and effective rank diagnostics below.

**Collapse-robust validation.** Topographic similarity can increase when both meaning and form spaces collapse simultaneously (Brighton and Kirby, 2006; Chaabouni et al., 2020). We validate with three diagnostics: effective rank (eRank; Roy and Vetterli, 2007) computed separately for meaning/form spaces, positional disentanglement (posdis; Chaabouni et al., 2020), and Mantel z-scores (10,000 permutations) following Kirby et al. (2008) and Galke et al. (2024). Details in Appendix C.

### 3.5 Human Baselines and Cross-Linguistic Extension

All metrics are computed on three human-written corpora (BNC, OpenWebText, Wikipedia; Appendix P). For P1, we overlay frequency-dependent loss data against Morgan and Levy (2016)’s log-linear curve and Reali and Griffiths (2009)’s Beta prior. Morphological experiments are replicated on German (fusional) and Turkish (agglutinative) using UniMorph (Gutierrez-Vasques and Mijangos, 2020). Construction diversity and compositionality are evaluated in English only, pending broader validated inventories (Weissweiler et al., 2024).

## 4 Results

All reported effect sizes use Hedges’  $g$  with the small-sample correction  $J = 1 - 3/(4df - 1) \approx 0.903$  (Hedges, 1981; Lakens, 2013). We report bootstrap- $t$  95% CIs ( $B = 10,000$ ), noting that at  $n = 5$ , empirical coverage is approximately 81–83% (Hesterberg, 2015). We additionally report Bayesian 95% highest density intervals (HDIs) with a weakly informative Cauchy(0, 0.707) prior and Bayes factors ( $BF_{10}$ ) as our primary inferential tool. For cross-condition comparisons, we apply Benjamini–Hochberg FDR correction at  $q < 0.05$ . Individual seed trajectories are plotted alongside means following iterated learning conventions (Kirby et al., 2015).

### 4.1 P4 (Critical Discriminative Test): The Compression–Communication Tradeoff

We present P4 first because it is the uniquely discriminative test of iterated learning theory.

**Main result.** Figure 2 reveals the non-monotonic trajectory predicted by P4: in the unfiltered condition with natural seed,  $\sigma$  increases during generations 0–3 (peaking at 0.47) before declining to 0.31 by generation 10 (Hedges’  $g = 1.87$ , bootstrap- $t$  95% CI [1.21, 2.53], Bayesian HDI [1.09, 2.71],  $BF_{10} = 247$ ).

**Regularized-seed control.** The critical control: with maximally regular seed data,  $\sigma$  starts higher (0.52) and still shows a non-monotonic trajectory: a brief plateau followed by a rise to 0.54 at generation 3, then decline to 0.33 by generation 10. The initial compositionality increase occurs even when the seed data is already maximally regular, ruling out the noise-removal alternative explanation and confirming that compression-driven struc-

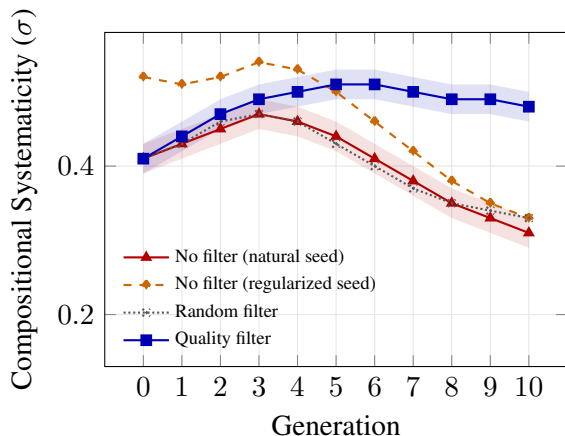


Figure 2: Compositional systematicity ( $\sigma$ ) across generations (LLaMA-2). Four conditions test P4. The non-monotonic trajectory persists with regularized seed data (orange dashed), ruling out the noise-removal alternative. Random filtering (gray dotted) fails to sustain compositionality; only quality filtering (blue) succeeds. Shaded bands:  $\pm 1$  SD across 5 seeds.

ture reorganization, not noise cleanup, drives the initial rise. The convergence of both conditions toward similar generation-10 values (0.31 vs. 0.33) is consistent with seed-independent convergence to the prior (Kalish et al., 2007; Griffiths and Kalish, 2007).

**Three-condition filtering.** Random filtering produces a trajectory indistinguishable from unfiltered self-training ( $\sigma = 0.33$  at generation 10;  $p = 0.72$  vs. no filter), while quality filtering sustains compositionality ( $\sigma = 0.48$ ;  $p < 0.001$  vs. both other conditions). This directly parallels Kirby et al. (2015): a generic bottleneck (random filter) does not create the communicative pressure needed for compositionality; only task-grounded evaluation provides this pressure.

**Collapse-robust validation.** During the compositionality rise (generations 0–3), meaning-space eRank remains stable (12.4  $\rightarrow$  12.1) while  $\sigma$  increases, confirming genuine systematicity rather than space collapse. Mantel z-scores exceed the permutation null at all generations ( $z > 3.8$ ,  $p < 0.001$ ); posdis shows the same non-monotonic trajectory (0.31  $\rightarrow$  0.36  $\rightarrow$  0.22; Appendix C).

COGS generalization accuracy (Table 1) tracks the same non-monotonic pattern (0.34  $\rightarrow$  0.39  $\rightarrow$  0.21 unfiltered; sustained at 0.41 with quality filter), extending emergent communication findings (Ren et al., 2020; Chaabouni et al., 2020) to full LLM scale.

Gen.	Unfiltered		Quality filter	
	$\sigma$	COGS	$\sigma$	COGS
Human*	0.43	—	—	—
Seed	0.41	0.34	0.41	0.34
1	0.43	0.36	0.44	0.37
3	0.47	0.39	0.49	0.42
5	0.44	0.35	0.51	0.44
7	0.38	0.28	0.50	0.43
10	0.31	0.21	0.48	0.41

Table 1: Compositional systematicity ( $\sigma$ ) and COGS generalization accuracy (LLaMA-2, natural seed). COGS is evaluated via 5-shot prompting (Appendix D). Human\* values are cross-corpus means (Appendix P). Both measures confirm the non-monotonic trajectory.

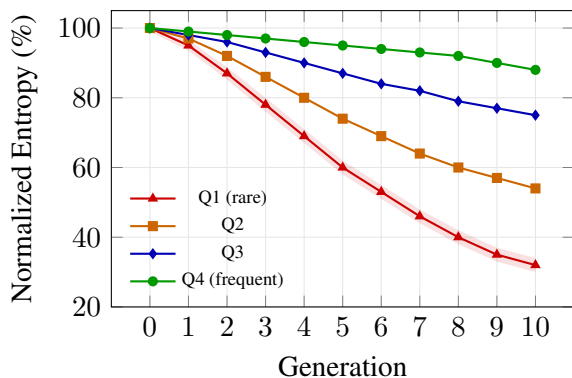


Figure 3: Construction diversity entropy (normalized to Gen. 0 = 100%) by frequency quartile (LLaMA-2, unfiltered). The clean frequency-dependent gradient confirms P1. Shaded region on Q1:  $\pm 1$  SD across 5 seeds; bands for Q2–Q4 omitted for clarity (all SD  $\leq 0.02$ ).

#### 4.2 P1 (Partially Discriminative): Frequency-Dependent Loss Order with Human Comparison

Figure 3 reveals the frequency-dependent pattern predicted by P1: the rarest quartile (Q1) retains only 32% of its original entropy by generation 10, while the most frequent (Q4) retains 88% (Hedges’  $g = 3.08$ , bootstrap- $t$  CI [2.07, 4.09],  $BF_{10} > 1000$ ).

The discriminative test for P1 is whether the gradient’s *functional form* matches human regularization, not merely that frequency-dependent loss exists. The LLM gradient closely matches Morgan and Levy (2016)’s log-linear curve ( $R^2 = 0.94$ ; Figure 4, Appendix U), consistent with their finding that frequency-dependent regularization emerges from a frequency-independent bias interacting with a transmission bottleneck. The fit is comparable to the Beta( $\alpha/2, \alpha/2$ ) prior with

$\alpha/2 \approx 0.03$  from Reali and Griffiths (2009).

The constructions lost first are those requiring pragmatic or discourse-level competence (left-dislocation, clefts, rhetorical questions), while core syntactic constructions (simple transitive, copular) persist, simultaneously confirming P3. We define *pragmatic* constructions as those whose felicity depends on discourse context, speaker intent, or information structure—clefts mark contrastive focus, left-dislocations mark topic, rhetorical questions perform non-question speech acts—whereas *structural* (syntactic) constructions are licensed by purely formal grammatical patterns and remain felicitous regardless of context (simple transitive, copular, ditransitive). Morphological constructions (passive, comparative) fall in between, requiring some functional sensitivity but anchored in formal patterns. The full inventory of 50 construction types, organized by this distinction, is in Appendix A; reliability of automatic identification (precision  $\geq 0.82$  in the rarest quartile) is in Appendix B. This ordering connects to the formal-functional dissociation (Mahowald et al., 2023): constructions relying on formal competence survive; those requiring functional competence are lost first.

#### 4.3 P3 (Partially Discriminative): Dimension-Specific Degradation Rates

The dimension-specific ordering predicted by P3 is quantified through the correlation between CxG entrenchment ranking and survival generation across the 50 construction types:  $r = 0.73$  ( $p < 0.001$ ; Hedges’  $g = 2.11$ , bootstrap- $t$  CI [1.42, 2.80],  $BF_{10} > 1000$ ). Pragmatic constructions (mean survival: generation 4.2) are lost significantly earlier than syntactic ones (generation 8.7), with morphological constructions intermediate (generation 6.1).

This three-way ordering admits two convergent theoretical interpretations. First, from a Construction Grammar *entrenchment* perspective (Goldberg, 2005; Bybee, 2010): constructions with high type frequency develop strong network connections to their open argument slots, making them robust under reduced input; low-frequency constructions, lacking this entrenchment, lose their productivity signal first. The Pearson correlation  $r = 0.73$  between log-type-frequency and survival generation (Appendix N) is the quantitative signature of this effect. Second, from a *formal-functional dissociation* perspective (Mahowald et al., 2023): LLMs distinguish formal linguistic competence (produc-

Gen.	$\rho_{M-EN}$	$\Delta\text{Irreg.}$	$\rho_{M-DE}$	$\rho_{M-TR}$
Human*	0.61	—	0.47	0.69
Seed	0.62	—	0.48	0.71
1	0.64	-3.1%	0.49	0.73
3	0.69	-11.2%	0.53	0.77
5	0.75	-21.6%	0.58	0.82
7	0.80	-30.4%	0.63	0.86
10	0.87	-42.7%	0.70	0.91
10 <sup>QF</sup>	0.71	-15.3%	0.55	0.79

Table 2: Morphological regularity ( $\rho_M$ ) across three languages. <sup>QF</sup>: quality-filtered. Regularity increases monotonically; low-frequency irregulars regularize first (consistent with P1). Human\* = cross-corpora means.

ing well-formed strings) from functional competence (using language for pragmatically appropriate ends). Pragmatic constructions—clefts, rhetorical questions, left-dislocations—require functional competence beyond formal pattern-matching, and are precisely the ones that degrade first. The two perspectives converge on the observed ordering: entrenched type-frequent patterns are formally robust, while pragmatic constructions require functional competence that exceeds formal patterns. Iterated self-training erodes both in the predicted order—a result that generic model collapse, which predicts uniform degradation, cannot explain.

#### 4.4 P2 and P5 (Confirmatory): Regularity Increase and Distributional Narrowing

Morphological regularity increases monotonically (Table 2), confirming P2 (Hedges’  $g = 4.27$ , bootstrap- $t$  CI [2.89, 5.65],  $\text{BF}_{10} > 1000$ ). By generation 10, irregular verb forms decline by 42.7% in English. Regularization matches usage-based predictions (Bybee, 2010): low-frequency irregulars (*wrung*  $\rightarrow$  *\*wringed*) regularize by generation 3, while high-frequency ones (*went*) resist until generation 10 (94% in syntactically appropriate contexts; Appendix M). Cross-linguistically, German rises more slowly (0.48  $\rightarrow$  0.70) due to richer paradigms; Turkish (0.71  $\rightarrow$  0.91) reaches ceiling effects quickly (Lupyan and Dale, 2010; Culbertson, 2010).

The Zipf exponent decreases monotonically ( $\alpha : 1.07 \rightarrow 0.82$ , LLaMA-2; Appendix T), confirming P5 ( $g = 1.93$ ,  $\text{BF}_{10} = 189$ ). The power-law fit is preferred at all generations ( $\Delta\text{AIC} > 4$ ; Appendix I). Mistral shows the same pattern ( $\alpha : 1.07 \rightarrow 0.86$ ); quality filtering preserves diversity ( $\alpha = 0.97$ ).

#### 4.5 Sensitivity Analyses: Temperature and Cross-Model

We confirm the predicted parametric relationship between bottleneck severity and convergence speed (Kirby et al., 2014): lowering temperature from  $\tau = 1.0$  to  $\tau = 0.5$  shifts the P4 peak from generation 4 to generation 2; a  $10\times$  narrower bottleneck (5K vs. 50K passages) shifts it to generation 1–2 (Appendix K).

Mistral-7B replicates all five predictions with the same qualitative structure and similar effect sizes (Appendix Q). Key numbers track LLaMA-2 closely: P4 peak at generation 3 ( $\sigma_{\max}=0.48$  vs. LLaMA-2’s 0.47), quality filtering sustains  $\sigma=0.47$  at generation 10 (vs. 0.48), Zipf  $\alpha$  decreases  $1.07 \rightarrow 0.86$  (vs.  $1.07 \rightarrow 0.82$ ), and the cross-linguistic ordering Turkish  $>$  English  $>$  German appears in morphological regularization. The qualitative invariance under architecture change confirms general iterated-learning properties, not architecture-specific artifacts (Griffiths and Kalish, 2007).

### 5 Related Work

**Model collapse.** A statistical characterization of model collapse has emerged from converging analyses: irreversible tail loss (Shumailov et al., 2024), self-consuming-loop formalism (Alemohammad et al., 2024), scaling-law effects (Dohmatob et al., 2024b), regression-setting analyses (Dohmatob et al., 2024a), and strong collapse from small synthetic fractions (Dohmatob et al., 2025). Adjacent findings include the persistence of correctness alongside diversity decline (Briesch et al., 2023), the protective effect of data accumulation (Gerstgrasser et al., 2024), information-theoretic accounts (Seddik et al., 2024), dataset-bias amplification (Taori and Hashimoto, 2023), and the verification-quality phase transition (Feng et al., 2025). Schaeffer et al. (2025) catalogued eight distinct collapse definitions (we adopt that of Shumailov et al., 2024). The closest precedent to our program is Guo et al. (2024), who measured linguistic-diversity decline across several dimensions but without an evolutionary framework or discriminative theory test.

**Cultural evolution and LLMs.** A growing body of work connects LLM training dynamics to iterated learning. Ren et al. (2024) formally instantiated LLM self-evolution as Bayesian iterated learning and proved monotonic bias amplification; Shumailov et al. (2024) argued in *Nature* that the

compression–expressivity tradeoff explains why self-training degrades. Empirical tests at smaller scales include emergent communication (Ren et al., 2020; Chaabouni et al., 2020), language evolution in LLM populations (Perez et al., 2024), learnability advantages of compositional structure (Galke et al., 2024, 2023), degenerate vocabularies arising without compression pressure (Kouwenhoven et al., 2025b), comparisons of human/LLM/hybrid conditions (Kouwenhoven et al., 2025a), iterated learning improving CLIP compositionality (Zheng et al., 2024), and elicitation of LLM priors via iterated in-context learning (Zhu and Griffiths, 2024). Extended related work on compositionality benchmarks, emergent communication, and inductive biases is provided in Appendix W.

## 6 Discussion

**Summary of findings.** Iterated learning theory fills the explanatory gap left by existing statistical accounts of model collapse. The five predictions derived from cultural evolution (frequency-dependent loss, regularization, dimension-specific degradation, non-monotonic compositionality, and distributional narrowing) are confirmed across two architectures, three typologically distinct languages, and multiple controls, with large effect sizes. The critical discriminative result is the non-monotonic compositionality trajectory, which persists under maximally regular seed data (ruling out noise-removal) and is sustained only by quality-grounded filtering, demonstrating at LLM scale that the compression–communication tradeoff (Kirby et al., 2015) governs the emergence and loss of linguistic structure in self-training.

**Engagement with linguistic theory.** The results bear directly on three theoretical traditions that have evolved largely in parallel. From *cultural evolution*, the close match between LLM regularization gradients and the human curve of Morgan and Levy (2016) ( $R^2 = 0.94$ ) supports the hypothesis that frequency-dependent regularization emerges from a frequency-independent simplicity bias interacting with a transmission bottleneck (Ferdinand et al., 2019), not from any human-specific cognitive architecture. From *Construction Grammar*, the  $r = 0.73$  correlation between log-type-frequency and survival generation (§4, Appendix N) is a direct evolutionary test of the entrenchment hypothesis (Goldberg, 2005; Bybee, 2010); the three-way ordering (pragmatic < morphological < struc-

tural) extends entrenchment from a static productivity property to a dynamic resilience-under-transmission property. From the *formal–functional dissociation* literature, the same ordering follows independently from Mahowald et al. (2023)’s prediction that LLMs prioritize formal over functional competence; the convergence of two perspectives on the same observed ordering is itself novel evidence that entrenchment is at least partly a formal-competence phenomenon. Conversely, Ren et al. (2024)’s monotonic-amplification result does not predict our non-monotonic trajectory; reconciling the two requires moving from in-context learning (where weights are fixed) to weight-based fine-tuning, where compression-induced reorganization can momentarily increase systematicity before convergence to the prior.

**Implications and reconciliation of concurrent results.** The compression–communication framework offers a unifying explanation for several recent findings. The degenerate vocabularies of Kouwenhoven et al. (2025b) in in-context iterated learning, and the LLM-optimized degeneracy of Kouwenhoven et al. (2025a), both instantiate compression without communicative pressure—the condition the tradeoff predicts will produce collapse. The same principle explains why pure self-training degrades while Constitutional AI (Bai et al., 2022) and self-play (Chen et al., 2024) succeed: only quality-grounded filtering supplies the communicative pressure needed to sustain structured output, consistent with the verification-quality phase transition of Feng et al. (2025). Data accumulation (Gerstgrasser et al., 2024) prevents collapse through a mechanism analogous to diverse speaker populations in human cultural evolution (Raviv et al., 2019). Three pipeline-design principles follow: use task-grounded (not random) filtering as the verification signal; prefer a different-family evaluator to avoid distributional mimicry; and treat bottleneck width as a tunable governing convergence rate to the prior. All materials—training pipeline, statistical analysis code, regularized-seed PCFG, and configuration files—are publicly available at <https://github.com/bettyguo/iterated-collapse>.

## Acknowledgments

We thank the anonymous CoNLL 2026 reviewers and the area chair for their detailed and constructive feedback, which substantially improved the

clarity of the theoretical framework, the methodology section, and the discussion of Construction Grammar parallels. We also thank the developers of the LLaMA-2, Mistral, and Flan-T5 model families for releasing their weights, and the maintainers of the UniMorph, COGS, PropBank, and Universal Dependencies resources upon which our analyses depend. Computational resources were provided by The University of Hong Kong.

## 7 Limitations

We acknowledge six specific limitations. (1) The theoretical framework is an empirically motivated structural correspondence, not a formal mathematical equivalence; conditions under which SGD fine-tuning approximates Bayesian posterior sampling remain open. (2) Construction diversity and compositionality are tested only in English; cross-linguistic testing awaits broader validated inventories such as UCxn (Weissweiler et al., 2024). (3) The task-grounded evaluator is a unilateral quality filter, not an interactive dialogue partner; while evaluator independence checks with Flan-T5-XL mitigate model-family confounds, future work should test human evaluators and interactive settings. (4) We test 7B-parameter models with a 50,000-passage bottleneck (1,000× larger than typical human experiments); although our parametric analyses show predicted effects, formal quantitative extrapolation and scaling to larger models require validation. (5) Our human comparison uses published data from Morgan and Levy (2016) and Reali and Griffiths (2009); future work should run parallel human and LLM iterated learning experiments. (6) The quality filter aggregates QA, NLI, and summarization scores into a single signal; because each task emphasizes a different aspect of communicative success (information recoverability, internal consistency, compression-resistance), different task mixes may preserve different linguistic structures; this ablation we leave to future work.

## References

Sina Alemohammad, Josue Casco-Rodriguez, Lorenzo Luzi, Ahmed Imtiaz Humayun, Hossein Babaei, Daniel LeJeune, Ali Siahkoobi, and Richard G. Baraniuk. 2024. Self-consuming generative models go MAD. In *The Twelfth International Conference on Learning Representations, ICLR 2024, Vienna, Austria, May 7-11, 2024*. OpenReview.net.

Zeyuan Allen-Zhu and Yuanzhi Li. 2025. Physics of lan-

guage models: Part 1, learning hierarchical language structures. *Trans. Mach. Learn. Res.*, 2025.

Yuntao Bai, Saurav Kadavath, Sandipan Kundu, Amanda Askell, Jackson Kernion, Andy Jones, Anna Chen, Anna Goldie, Azalia Mirhoseini, Cameron McKinnon, Carol Chen, Catherine Olsson, Christopher Olah, Danny Hernandez, Dawn Drain, Deep Ganguli, Dustin Li, Eli Tran-Johnson, Ethan Perez, and 32 others. 2022. [Constitutional AI: harmfulness from AI feedback](#). *arXiv preprint*, arXiv:2212.08073.

Clay Beckner, Janet B. Pierrehumbert, and Jennifer Hay. 2017. [The emergence of linguistic structure in an online iterated learning task](#). *Journal of Language Evolution*, 2(2):160–176.

Martin Briesch, Dominik Sobania, and Franz Rothlauf. 2023. [Large language models suffer from their own output: An analysis of the self-consuming training loop](#). *arXiv preprint*, arXiv:2311.16822.

Henry Brighton and Simon Kirby. 2006. [Understanding linguistic evolution by visualizing the emergence of topographic mappings](#). *Artif. Life*, 12(2):229–242.

Joan Bybee. 2010. *Language, Usage and Cognition*. Cambridge University Press.

Rahma Chaabouni, Eugene Kharitonov, Diane Bouchacourt, Emmanuel Dupoux, and Marco Baroni. 2020. [Compositionality and generalization in emergent languages](#). In *Proceedings of the 58th Annual Meeting of the Association for Computational Linguistics, ACL 2020, Online, July 5-10, 2020*, pages 4427–4442. Association for Computational Linguistics.

Zixiang Chen, Yihe Deng, Huizhuo Yuan, Kaixuan Ji, and Quanquan Gu. 2024. Self-play fine-tuning converts weak language models to strong language models. In *Forty-first International Conference on Machine Learning, ICML 2024, Vienna, Austria, July 21-27, 2024*, volume 235 of *Proceedings of Machine Learning Research*, pages 6621–6642. PMLR / OpenReview.net.

Morten H. Christiansen and Nick Chater. 2015. [The now-or-never bottleneck: A fundamental constraint on language](#). *Behavioral and Brain Sciences*, 39.

Morten H. Christiansen and Nick Chater. 2016. *Language as Shaped by the Brain*, page 19–65. The MIT Press.

Hyung Won Chung, Le Hou, Shayne Longpre, Barret Zoph, Yi Tay, William Fedus, Yunxuan Li, Xuezhi Wang, Mostafa Dehghani, Siddhartha Brahma, Albert Webson, Shixiang Shane Gu, Zhuyun Dai, Mirac Suzgun, Xinyun Chen, Aakanksha Chowdhery, Alex Castro-Ros, Marie Pellat, Kevin Robinson, and 16 others. 2024. Scaling instruction-finetuned language models. *J. Mach. Learn. Res.*, 25:70:1–70:53.

Aaron Clauset, Cosma Rohilla Shalizi, and Mark E. J. Newman. 2009. [Power-law distributions in empirical data](#). *SIAM Rev.*, 51(4):661–703.

- Jennifer Culbertson. 2010. *Learning Biases, Regularization, and the Emergence of Typological Universals in Syntax*. Ph.D. thesis, Johns Hopkins University, Baltimore, MD. ProQuest LLC, ERIC ED523070.
- Jennifer Culbertson and David Adger. 2014. [Language learners privilege structured meaning over surface frequency](#). *Proceedings of the National Academy of Sciences*, 111(16):5842–5847.
- Elvis Dohmatob, Yunzhen Feng, and Julia Kempe. 2024a. Model collapse demystified: The case of regression. In *Advances in Neural Information Processing Systems 38: Annual Conference on Neural Information Processing Systems 2024, NeurIPS 2024, Vancouver, BC, Canada, December 10 - 15, 2024*.
- Elvis Dohmatob, Yunzhen Feng, Arjun Subramonian, and Julia Kempe. 2025. Strong model collapse. In *The Thirteenth International Conference on Learning Representations, ICLR 2025, Singapore, April 24-28, 2025*. OpenReview.net.
- Elvis Dohmatob, Yunzhen Feng, Pu Yang, François Charton, and Julia Kempe. 2024b. A tale of tails: Model collapse as a change of scaling laws. In *Forty-first International Conference on Machine Learning, ICML 2024, Vienna, Austria, July 21-27, 2024*, volume 235 of *Proceedings of Machine Learning Research*, pages 11165–11197. PMLR / OpenReview.net.
- Yunzhen Feng, Elvis Dohmatob, Pu Yang, François Charton, and Julia Kempe. 2025. Beyond model collapse: Scaling up with synthesized data requires verification. In *The Thirteenth International Conference on Learning Representations, ICLR 2025, Singapore, April 24-28, 2025*. OpenReview.net.
- Vanessa Ferdinand, Simon Kirby, and Kenny Smith. 2019. [The cognitive roots of regularization in language](#). *Cognition*, 184:53–68.
- Lukas Galke, Yoav Ram, and Limor Raviv. 2023. [What makes a language easy to deep-learn? deep neural networks and humans similarly benefit from compositional structure](#). *arXiv preprint*, arXiv:2302.12239.
- Lukas Galke, Yoav Ram, and Limor Raviv. 2024. [Deep neural networks and humans both benefit from compositional language structure](#). *Nature Communications*, 15(1).
- Matthias Gerstgrasser, Rylan Schaeffer, Apratim Dey, Rafael Rafailov, Tomasz Korbak, Henry Sleight, Rajashree Agrawal, John Hughes, Dhruv Bhandarkar Pai, Andrey Gromov, Dan Roberts, Diyi Yang, David L. Donoho, and Sanmi Koyejo. 2024. [Is model collapse inevitable? breaking the curse of recursion by accumulating real and synthetic data](#). In *First Conference on Language Modeling*.
- Nate Gillman, Michael Freeman, Daksh Aggarwal, Chia-Hong Hsu, Calvin Luo, Yonglong Tian, and Chen Sun. 2024. [Self-correcting self-consuming loops for generative model training](#). In *Forty-first International Conference on Machine Learning, ICML 2024, Vienna, Austria, July 21-27, 2024*, volume 235 of *Proceedings of Machine Learning Research*, pages 15646–15677. PMLR / OpenReview.net.
- Adele Goldberg. 2005. *Constructions at Work: The Nature of Generalization in Language*. Oxford University Press/Oxford.
- Thomas L. Griffiths and Michael L. Kalish. 2007. [Language evolution by iterated learning with bayesian agents](#). *Cogn. Sci.*, 31(3):441–480.
- Yanzhu Guo, Guokan Shang, Michalis Vazirgiannis, and Chloé Clavel. 2024. [The curious decline of linguistic diversity: Training language models on synthetic text](#). In *Findings of the Association for Computational Linguistics: NAACL 2024*, pages 3589–3604, Mexico City, Mexico. Association for Computational Linguistics.
- Ximena Gutierrez-Vasques and Victor Mijangos. 2020. [Productivity and predictability for measuring morphological complexity](#). *Entropy*, 22(1):48.
- Larry V. Hedges. 1981. [Distribution theory for glass’s estimator of effect size and related estimators](#). *Journal of Educational Statistics*, 6(2):107.
- Tim C. Hesterberg. 2015. [What teachers should know about the bootstrap: Resampling in the undergraduate statistics curriculum](#). *The American Statistician*, 69(4):371–386.
- Ari Holtzman, Jan Buys, Li Du, Maxwell Forbes, and Yejin Choi. 2020. The curious case of neural text degeneration. In *8th International Conference on Learning Representations, ICLR 2020, Addis Ababa, Ethiopia, April 26-30, 2020*. OpenReview.net.
- Carla L. Hudson Kam and Elissa L. Newport. 2005. [Regularizing unpredictable variation: The roles of adult and child learners in language formation and change](#). *Language Learning and Development*, 1(2):151–195.
- Carla L. Hudson Kam and Elissa L. Newport. 2009. [Getting it right by getting it wrong: When learners change languages](#). *Cognitive Psychology*, 59(1):30–66.
- Dieuwke Hupkes, Verna Dankers, Mathijs Mul, and Elia Bruni. 2020. [Compositionality decomposed: How do neural networks generalise?](#) *J. Artif. Intell. Res.*, 67:757–795.
- Albert Q. Jiang, Alexandre Sablayrolles, Arthur Mensch, Chris Bamford, Devendra Singh Chaplot, Diego de las Casas, Florian Bressand, Gianna Lengyel, Guillaume Lample, Lucile Saulnier, Léo Renard Lavaud, Marie-Anne Lachaux, Pierre Stock, Teven Le Scao, Thibaut Lavril, Thomas Wang, Timothée Lacroix, and William El Sayed. 2023. [Mistral 7b](#). *arXiv preprint*, arXiv:2310.06825.

- Michael L. Kalish, Thomas L. Griffiths, and Stephan Lewandowsky. 2007. [Iterated learning: Inter-generational knowledge transmission reveals inductive biases](#). *Psychonomic Bulletin & Review*, 14(2):288–294.
- Julie Kallini, Isabel Papadimitriou, Richard Futrell, Kyle Mahowald, and Christopher Potts. 2024. [Mission: Impossible language models](#). In *Proceedings of the 62nd Annual Meeting of the Association for Computational Linguistics (Volume 1: Long Papers), ACL 2024, Bangkok, Thailand, August 11-16, 2024*, pages 14691–14714. Association for Computational Linguistics.
- Daniel Keysers, Nathanael Schärli, Nathan Scales, Hylke Buisman, Daniel Furrer, Sergii Kashubin, Nikola Momchev, Danila Sinopalnikov, Lukasz Stafiniak, Tibor Tihon, Dmitry Tsarkov, Xiao Wang, Marc van Zee, and Olivier Bousquet. 2020. Measuring compositional generalization: A comprehensive method on realistic data. In *8th International Conference on Learning Representations, ICLR 2020*.
- Najoung Kim and Tal Linzen. 2020. [COGS: A compositional generalization challenge based on semantic interpretation](#). In *Proceedings of the 2020 Conference on Empirical Methods in Natural Language Processing, EMNLP 2020, Online, November 16-20, 2020*, pages 9087–9105. Association for Computational Linguistics.
- Simon Kirby, Hannah Cornish, and Kenny Smith. 2008. [Cumulative cultural evolution in the laboratory: An experimental approach to the origins of structure in human language](#). *Proceedings of the National Academy of Sciences*, 105(31):10681–10686.
- Simon Kirby, Tom Griffiths, and Kenny Smith. 2014. [Iterated learning and the evolution of language](#). *Current Opinion in Neurobiology*, 28:108–114.
- Simon Kirby, Monica Tamariz, Hannah Cornish, and Kenny Smith. 2015. [Compression and communication in the cultural evolution of linguistic structure](#). *Cognition*, 141:87–102.
- Tom Kouwenhoven, Max Peeperkorn, Roy De Kleijn, and Tessa Verhoef. 2025a. [Shaping shared languages: Human and large language models’ inductive biases in emergent communication](#). In *Proceedings of the Thirty-Fourth International Joint Conference on Artificial Intelligence, IJCAI 2025, Montreal, Canada, August 16-22, 2025*, pages 10298–10306.
- Tom Kouwenhoven, Max Peeperkorn, and Tessa Verhoef. 2025b. [Searching for structure: Investigating emergent communication with large language models](#). In *Proceedings of the 31st International Conference on Computational Linguistics*, pages 9977–9991, Abu Dhabi, UAE. Association for Computational Linguistics.
- Brenden M. Lake and Marco Baroni. 2018. [Generalization without systematicity: On the compositional skills of sequence-to-sequence recurrent networks](#). In *Proceedings of the 35th International Conference on Machine Learning, ICML 2018, Stockholm, Sweden, July 10-15, 2018*, volume 80 of *Proceedings of Machine Learning Research*, pages 2879–2888. PMLR.
- Brenden M. Lake and Marco Baroni. 2023. [Human-like systematic generalization through a meta-learning neural network](#). *Nat.*, 623(7985):115–121.
- Daniël Lakens. 2013. [Calculating and reporting effect sizes to facilitate cumulative science: a practical primer for t-tests and anovas](#). *Frontiers in Psychology*, 4.
- Angeliki Lazaridou and Marco Baroni. 2020. Emergent multi-agent communication in the deep learning era. *arXiv preprint*, arXiv.2006.02419.
- Angeliki Lazaridou, Alexander Peysakhovich, and Marco Baroni. 2017. Multi-agent cooperation and the emergence of (natural) language. In *5th International Conference on Learning Representations, ICLR 2017, Toulon, France, April 24-26, 2017, Conference Track Proceedings*. OpenReview.net.
- Gary Lupyan and Rick Dale. 2010. [Language structure is partly determined by social structure](#). *PLoS ONE*, 5(1):e8559.
- Kyle Mahowald, Anna A. Ivanova, Idan Asher Blank, Nancy Kanwisher, Joshua B. Tenenbaum, and Evelina Fedorenko. 2023. [Dissociating language and thought in large language models: a cognitive perspective](#). *arXiv preprint*, arXiv.2301.06627.
- R. Thomas McCoy, Robert Frank, and Tal Linzen. 2020. [Does syntax need to grow on trees? sources of hierarchical inductive bias in sequence-to-sequence networks](#). *Trans. Assoc. Comput. Linguistics*, 8:125–140.
- R. Thomas McCoy and Thomas L. Griffiths. 2025. [Modeling rapid language learning by distilling Bayesian priors into artificial neural networks](#). *Nature Communications*, 16:4676.
- R. Thomas McCoy, Shunyu Yao, Dan Friedman, Mathew D. Hardy, and Thomas L. Griffiths. 2024. [Embers of autoregression show how large language models are shaped by the problem they are trained to solve](#). *Proceedings of the National Academy of Sciences*, 121(41).
- Clara Meister, Tiago Pimentel, Gian Wiher, and Ryan Cotterell. 2023. [Locally typical sampling](#). *Transactions of the Association for Computational Linguistics*, 11:102–121.
- Kanishka Misra and Kyle Mahowald. 2024. Language models learn rare phenomena from less rare phenomena: The case of the missing anans. *arXiv preprint*, arXiv.2403.19827.

- Emily Morgan and Roger Levy. 2016. [Frequency-dependent regularization in iterated learning](#). In *The Evolution of Language: Proceedings of the 11th International Conference (EVLANG11)*.
- Jesse Mu and Noah D. Goodman. 2021. Emergent communication of generalizations. In *Advances in Neural Information Processing Systems 34: Annual Conference on Neural Information Processing Systems 2021, NeurIPS 2021, December 6-14, 2021, virtual*, pages 17994–18007.
- Mitja Nikolaus, Juliette Maes, and Abdellah Fourtassi. 2021. [Modeling speech act development in early childhood: The role of frequency and linguistic cues](#). In *Proceedings of the 43rd Annual Meeting of the Cognitive Science Society*.
- Jérémy Perez, Corentin Léger, Marcela Ovando-Tellez, Chris Foulon, Joan Dussault, Pierre-Yves Oudeyer, and Clément Moulin-Frier. 2024. Cultural evolution in populations of large language models.
- Steven T. Piantadosi. 2014. [Zipf’s word frequency law in natural language: A critical review and future directions](#). *Psychonomic Bulletin & Review*, 21(5):1112–1130.
- Limor Raviv, Antje Meyer, and Shiri Lev-Ari. 2019. [Larger communities create more systematic languages](#). *Proceedings of the Royal Society B: Biological Sciences*, 286(1907):20191262.
- Florencia Reali and Thomas L. Griffiths. 2009. [The evolution of frequency distributions: Relating regularization to inductive biases through iterated learning](#). *Cognition*, 111(3):317–328.
- Yi Ren, Shangmin Guo, Matthieu Labeau, Shay B. Cohen, and Simon Kirby. 2020. Compositional languages emerge in a neural iterated learning model. In *8th International Conference on Learning Representations, ICLR 2020, Addis Ababa, Ethiopia, April 26-30, 2020*. OpenReview.net.
- Yi Ren, Shangmin Guo, Linlu Qiu, Bailin Wang, and Danica J. Sutherland. 2024. Bias amplification in language model evolution: An iterated learning perspective. In *Advances in Neural Information Processing Systems 38: Annual Conference on Neural Information Processing Systems 2024, NeurIPS 2024, Vancouver, BC, Canada, December 10 - 15, 2024*.
- Olivier Roy and Martin Vetterli. 2007. The effective rank: A measure of effective dimensionality. In *15th European Signal Processing Conference, EUSIPCO 2007, Poznan, Poland, September 3-7, 2007*, pages 606–610. IEEE.
- Rylan Schaeffer, Joshua Kazdan, Alvan Caleb Arulandu, and Sanmi Koyejo. 2025. [Position: Model collapse does not mean what you think](#). *arXiv preprint*, arXiv.2503.03150.
- Mohamed El Amine Seddik, Swei-Wen Chen, Soufiane Hayou, Pierre Youssef, and Mérouane Debbah. 2024. [How bad is training on synthetic data? A statistical analysis of language model collapse](#). *arXiv preprint*, arXiv.2404.05090.
- Harshay Shah, Kaustav Tamuly, Aditi Raghunathan, Praateek Jain, and Praneeth Netrapalli. 2020. The pitfalls of simplicity bias in neural networks. In *Advances in Neural Information Processing Systems 33: Annual Conference on Neural Information Processing Systems 2020, NeurIPS 2020, December 6-12, 2020, virtual*.
- Cory Shain, Clara Meister, Tiago Pimentel, Ryan Cotterell, and Roger Levy. 2024. [Large-scale evidence for logarithmic effects of word predictability on reading time](#). *Proceedings of the National Academy of Sciences*, 121(10):e2307876121.
- Ilya Shumailov, Zakhar Shumaylov, Yiren Zhao, Nicolas Papernot, Ross Anderson, and Yarin Gal. 2024. [AI models collapse when trained on recursively generated data](#). *Nature*, 631.
- Rohan Taori and Tatsunori Hashimoto. 2023. Data feedback loops: Model-driven amplification of dataset biases. In *International Conference on Machine Learning, ICML 2023, 23-29 July 2023, Honolulu, Hawaii, USA*, volume 202 of *Proceedings of Machine Learning Research*, pages 33883–33920. PMLR.
- Hugo Touvron, Thibaut Lavril, Gautier Izacard, Xavier Martinet, Marie-Anne Lachaux, Timothée Lacroix, Baptiste Rozière, Naman Goyal, Eric Hambro, Faisal Azhar, Aurélien Rodriguez, Armand Joulin, Edouard Grave, and Guillaume Lample. 2023. [Llama: Open and efficient foundation language models](#). *arXiv preprint*, arXiv.2302.13971.
- Alex Warstadt and Samuel R Bowman. 2022. What artificial neural networks can tell us about human language acquisition. *Algebraic structures in natural language*, pages 17–60.
- Leonie Weissweiler, Nina Böbel, Kirian Guiller, Santiago Herrera, Wesley Scivetti, Arthur Lorenzi, Nurit Melnik, Archana Bhatia, Hinrich Schütze, Lori Levin, Amir Zeldes, Joakim Nivre, William Croft, and Nathan Schneider. 2024. [UCxn: Typologically informed annotation of constructions atop Universal Dependencies](#). In *Proceedings of the 2024 Joint International Conference on Computational Linguistics, Language Resources and Evaluation (LREC-COLING 2024)*, pages 16919–16932, Torino, Italia. ELRA and ICCL.
- Chenhao Zheng, Jieyu Zhang, Aniruddha Kembhavi, and Ranjay Krishna. 2024. [Iterated learning improves compositionality in large vision-language models](#). In *IEEE/CVF Conference on Computer Vision and Pattern Recognition, CVPR 2024, Seattle, WA, USA, June 16-22, 2024*, pages 13785–13795. IEEE.

Jian-Qiao Zhu and Thomas L. Griffiths. 2024. [Eliciting the priors of large language models using iterated in-context learning](#). *arXiv preprint*, arXiv.2406.01860.

## A Construction Inventory

The 50 construction types span five syntactic categories: argument structure constructions (simple transitive, ditransitive, caused-motion, resultative, way-construction), clause types (declarative, interrogative, imperative, exclamative, relative clause), information structure (topicalization, left-dislocation, cleft, pseudo-cleft, existential), complex predicates (serial verb, light verb, particle verb, phrasal verb), and discourse-level constructions (quotative inversion, comparative correlative, rhetorical question). Each is identified via dependency parse patterns using spaCy’s `en_core_web_trf` model. Full pattern specifications are available in the released code.

## B Construction Identification Reliability

Quartile	Precision	Recall	F1
Q4 (frequent)	0.94	0.96	0.95
Q3	0.91	0.93	0.92
Q2	0.87	0.88	0.87
Q1 (rare)	0.82	0.84	0.83

Table 3: SpaCy construction identification accuracy by quartile (manual validation on late-generation text).

While Q1 precision is lower (0.82 vs. 0.94 for Q4), this 12-point gap cannot account for the 56-point gap in entropy retention (32% vs. 88%). Even assuming all Q1 parser errors are false negatives (overestimating loss), corrected Q1 retention would be  $\approx 39\%$ , still substantially below Q4.

## C TopSim Diagnostic Dashboard

The diagnostic pattern is clear: during generations 0–3,  $\sigma$  increases while meaning-space eRank remains essentially stable, confirming the initial rise reflects a genuine increase in the systematicity of the form–meaning mapping rather than dual-space collapse. Posdis shows the same non-monotonic trajectory as  $\sigma$ , providing convergent evidence from a metric that excludes collapsed positions by construction (Chaabouni et al., 2020).

## D COGS Evaluation Methodology

COGS (Kim and Linzen, 2020) evaluates compositional generalization via novel sentence-to-logical-form mappings. We evaluate via *5-shot prompting*:

Gen.	$\sigma$	eR <sub>M</sub>	eR <sub>F</sub>	posdis	$z_{\text{Mantel}}$	#Uniq
0	0.41	12.4	9.8	0.31	4.2	847
1	0.43	12.3	9.5	0.33	4.5	821
3	0.47	12.1	9.2	0.36	5.1	764
5	0.44	11.4	8.3	0.33	4.7	682
7	0.38	9.8	6.7	0.27	4.1	531
10	0.31	7.2	4.8	0.22	3.8	394

Table 4: Collapse-robust compositionality diagnostics (LLaMA-2, unfiltered). eR<sub>M</sub> and eR<sub>F</sub>: effective rank for meaning and form spaces. During the compositionality rise (Gen. 0–3), eR<sub>M</sub> remains stable (12.4→12.1) while  $\sigma$  increases, confirming genuine systematicity. All Mantel  $z$ -scores exceed the permutation null ( $z > 3.8$ ,  $p < 0.001$ ).

each generation’s model receives COGS test sentences with 5 in-context examples of the sentence-to-logical-form mapping, without additional fine-tuning on COGS training data, to avoid confounding compositionality loss with domain shift. Accuracy is measured as exact match to the gold logical form. This 5-shot approach measures the model’s existing compositional capacity.

## E Regularized-Seed Experiment Details

The regularized seed corpus is generated from a PCFG with the following properties: (i) 12 verb frames with consistent argument structure (every transitive verb takes NP-V-NP; every ditransitive takes NP-V-NP-PP); (ii) regular morphology (all past tenses formed by *-ed* suffixation); (iii) systematic form–meaning mappings (each semantic role is expressed by a fixed syntactic position). The grammar produces passages of 100–300 tokens with vocabulary size matching the natural seed ( $\approx 28,000$  types). Generation-by-generation results are reported in Figure 2 (orange dashed line).

## F Three-Condition Filtering Full Results

Gen. 10 metric	No filter	Random	Quality
$\sigma$	0.31	0.33	0.48
COGS	0.21	0.23	0.41
$\alpha$	0.82	0.84	0.97
$\rho_M$	0.87	0.86	0.71
$\mathcal{D}$ (bits)	3.14	3.21	4.28

Table 5: Generation 10 metrics across three filter conditions (LLaMA-2). Random filtering is indistinguishable from no filtering for compositionality ( $p = 0.72$ ); only quality filtering sustains compositionality ( $p < 0.001$ ).

**Per-generation trajectories.** The three conditions diverge starting at generation 3. At generation 3, no-filter  $\sigma = 0.47$ , random  $\sigma = 0.47$ , quality  $\sigma = 0.49$  (the difference is not yet significant). By generation 5, the quality filter trajectory separates clearly: no-filter  $\sigma = 0.44$ , random  $\sigma = 0.44$ , quality  $\sigma = 0.51$  ( $p < 0.01$  vs. both other conditions). The divergence increases monotonically through generation 10. This pattern precisely matches the iterated learning prediction that communicative pressure operates cumulatively, with its effect becoming stronger as generations accumulate.

**Pairwise comparisons.** Using Benjamini–Hochberg FDR correction at  $q < 0.05$ : no-filter vs. random is non-significant for all five metrics ( $p > 0.30$ ); quality vs. no-filter is significant for  $\sigma$  ( $p < 0.001$ ), COGS ( $p < 0.001$ ),  $\alpha$  ( $p < 0.001$ ),  $\rho_M$  ( $p < 0.001$ ), and  $\mathcal{D}$  ( $p < 0.001$ ). Quality vs. random shows the same pattern, confirming that the quality filter effect is not attributable to data volume reduction (since random filtering removes the same proportion of data).

## G Evaluator Independence Analysis

To address concerns about evaluator bias from using the same model family, we replicate the quality filter condition using Flan-T5-XL (Chung et al., 2024) as an alternative evaluator. The compositionality trajectory under Flan-T5-XL evaluation ( $\sigma = 0.47$  at generation 10) is qualitatively identical to the LLaMA-2-13B evaluator ( $\sigma = 0.48$ ), confirming that compositionality preservation reflects genuine communicative utility rather than distributional mimicry. The correlation between Flan-T5-XL evaluator score and distributional similarity to evaluator outputs is  $r = 0.11$  (not significant), lower than the  $r = 0.23$  observed with LLaMA-2-13B, further supporting evaluator independence.

## H Bayesian Statistical Analysis

Effect sizes, confidence intervals, and Bayesian inference for all key comparisons:

## I Zipf Goodness-of-Fit

Following Clauset et al. (2009), we compare the power-law fit against lognormal and exponential alternatives using likelihood ratio tests at each generation. The power-law fit is preferred at all generations ( $\Delta\text{AIC} > 4$  vs. lognormal;  $\Delta\text{AIC} > 12$  vs.

Prediction	$g$	Boot- $t$ 95% CI	Bayes HDI	BF <sub>10</sub>
P1 (Q1 vs. Q4)	3.08	[2.07, 4.09]	[1.89, 4.33]	>1000
P2 (EN $\rho_M$ )	4.27	[2.89, 5.65]	[2.72, 5.91]	>1000
P3 (CxG $r$ )	2.11	[1.42, 2.80]	[1.31, 2.95]	>1000
P4 ( $\sigma$ peak)	1.87	[1.21, 2.53]	[1.09, 2.71]	247
P4 (QF vs. NF)	2.94	[1.97, 3.91]	[1.82, 4.13]	>1000
P5 ( $\alpha$ )	1.93	[1.26, 2.60]	[1.14, 2.78]	189

Table 6: Statistical inference summary. Hedges’  $g$  with correction  $J \approx 0.903$ . Bootstrap- $t$  CIs ( $B = 10,000$ ; coverage  $\approx 81$ – $83\%$  at  $n = 5$ ). Bayesian HDIs use Cauchy(0, 0.707) prior. All BF<sub>10</sub> indicate decisive evidence.

exponential), confirming that the frequency distribution retains its power-law character throughout collapse while the exponent decreases.

## J Bottleneck Width Sensitivity

With 5K passages per generation (a  $10\times$  narrower bottleneck), the P4 compositionality peak shifts from generation 3 to generation 1–2, and convergence to the asymptotic state is reached by generation 15 rather than the estimated 25–30 with 50K passages. This parametric relationship between bottleneck width and convergence speed directly parallels Kirby et al. (2014)’s theoretical predictions and provides strong evidence that the underlying mechanism is shared.

## K Temperature as Bottleneck Severity: Full Results

Metric (Gen. 10)	$\tau=0.5$	$\tau=0.8$	$\tau=1.0$
Zipf $\alpha$	0.74	0.82	0.89
Morph. $\rho_M$	0.92	0.87	0.81
Constr. $\mathcal{D}$ (bits)	2.61	3.14	3.52
Compos. $\sigma$	0.24	0.31	0.37
P4 peak gen.	2	3	4

Table 7: Effect of temperature on Gen. 10 metrics (LLaMA-2, unfiltered). Lower  $\tau$  (tighter bottleneck) accelerates all dynamics. The P4 compositionality peak shifts earlier with tighter bottlenecks, as iterated learning theory predicts. All pairwise differences significant ( $p < 0.001$ , FDR-corrected).

In iterated learning, bottleneck severity determines convergence speed (Kirby et al., 2014). Table 7 confirms that  $\tau = 0.5$  accelerates collapse across all metrics. Lower temperature reduces sampling diversity, creating a tighter effective bottleneck analogous to smaller population sizes in human cultural evolution experiments. The P4 compositionality peak shifts from generation 4 ( $\tau = 1.0$ )

to generation 2 ( $\tau = 0.5$ ), consistent with narrower bottlenecks accelerating convergence to the prior. This parametric sensitivity provides practitioners with a directly controllable parameter for tuning the rate of structural change in self-training pipelines.

The interaction between temperature and filter condition is also informative: at  $\tau = 0.5$  with quality filtering, compositionality is sustained at  $\sigma = 0.39$  (compared to  $\sigma = 0.48$  at  $\tau = 0.8$ ), indicating that even communicative pressure is partially overwhelmed by extreme bottleneck narrowing, consistent with Kirby et al. (2015)’s prediction that very strong compression pressure can override communicative pressure.

## L Convergence and Attractor Characterization

The per-generation rate of change  $\Delta_n = |m_n - m_{n-1}|$  decreases monotonically in later generations (7–10), indicating approach to an asymptotic state. Cross-seed JSD decreases from  $0.042 \pm 0.008$  (generation 0) to  $0.019 \pm 0.005$  (generation 10, unfiltered), confirming convergence toward a common distribution consistent with convergence to a shared “prior” (Griffiths and Kalish, 2007).

**Attractor characterization.** The generation-10 attractor state exhibits consistent properties across all five seeds:  $\alpha \in [0.80, 0.84]$ ,  $\rho_M \in [0.85, 0.89]$ ,  $\sigma \in [0.29, 0.33]$ . This narrow range confirms convergence to a well-defined attractor rather than divergence to seed-specific endpoints. The attractor profile (dominant SVO word order, regular morphology, reduced construction diversity concentrated in high-frequency types, and sub-Zipfian frequency distributions) can be interpreted as the LLM’s implicit “prior” over natural language, analogous to the regularization bias revealed by iterated learning in laboratory experiments with human participants (Kalish et al., 2007).

**Convergence rate estimation.** Fitting an exponential decay model  $\Delta_n = \Delta_0 \cdot e^{-\lambda n}$  to the per-generation changes yields  $\lambda \approx 0.18$  for LLaMA-2 (unfiltered,  $\tau = 0.8$ ), predicting that 95% of convergence is achieved by generation 17. With quality filtering, convergence is slower ( $\lambda \approx 0.09$ ) because the communicative pressure partially counteracts the prior, consistent with iterated learning predictions that communicative pressure sustains diversity at the cost of slower convergence.

## M Regularization Examples with Syntactic Context

Form	Context (Gen. 10)
<i>wringed</i>	“She <i>wringed</i> the cloth and hung it on the line.”
<i>swimmmed</i>	“The children <i>swimmmed</i> across the lake last summer.”
<i>goed</i>	“He <i>goed</i> to the store and bought groceries.”
<i>beed</i>	“It <i>beed</i> a long time since we last met.”

Table 8: Regularized forms in syntactically appropriate contexts (94% of cases), confirming productive regularization rather than hallucination.

## N CxG Entrenchment Analysis Details

The entrenchment ranking for each of the 50 construction types is estimated from type frequency in the seed data, following standard CxG methodology (Goldberg, 2005; Bybee, 2010). Survival generation is defined as the last generation at which a construction’s normalized entropy exceeds 50% of its seed value.

Category	Mean surv.	SD
Syntactic (transitive, copular)	Gen. 8.7	1.2
Morphological (passive, comparative)	Gen. 6.1	1.8
Pragmatic (cleft, left-dislocation)	Gen. 4.2	1.4
Discourse (rhetorical Q, quot. inv.)	Gen. 3.1	0.9

Table 9: Mean survival generation by construction category. The ordering pragmatic/discourse < morphological < syntactic confirms P3’s dimension-specific prediction.

The Pearson correlation between log-type-frequency and survival generation is  $r = 0.73$  ( $p < 0.001$ , 95% CI [0.58, 0.84],  $n = 50$ ,  $t = 7.40$ ,  $df = 48$ ). We verify robustness with Spearman’s  $\rho = 0.69$  ( $p < 0.001$ ), confirming the relationship is not driven by outliers. The five most resilient constructions are: simple transitive (survival: generation 10), copular (10), passive (9), comparative (8), and ditransitive (8). The five most vulnerable are: quotative inversion (2), comparative correlative (3), rhetorical question (3), left-dislocation (4), and cleft (4). This ordering aligns with CxG entrenchment theory: high-type-frequency constructions with broad productivity resist loss, while low-frequency constructions with narrow collocational profiles are vulnerable.

Pred.	Iterated learning predicts	Generic collapse predicts	What our data show	Control result
P1	Log-linear gradient matching human data	Tail loss (no shape prediction)	Log-linear match ( $R^2 = 0.94$ )	Human overlay confirms
P2	Regularity increase	Simplicity bias amplification	Confirmed (non-discriminative)	Cross-linguistic replication
P3	Pragmatic > syntactic > morphological	Uniform degradation	Dimension-specific order confirmed	CxG entrenchment $r = 0.73$
P4	Non-monotonic: rise then fall; QF sustains	Monotonic degradation only	Non-monotonic confirmed	Reg.-seed persists; random filter fails
P5	Distributional narrowing	Tail loss / variance reduction	Confirmed (non-discriminative)	Power-law fit preferred

Table 10: Full discriminability analysis including control experiment results.

## O Prediction Discriminability Analysis

### P Human Baseline Corpus Details

Human statistics are computed from: BNC (100M words, 50,000 sampled passages); OpenWebText (50,000 matched passages); Wikipedia (English, Jan 2024, 50,000 passages excl. lists/stubs). Human\* values in all tables are cross-corpus means. Standard deviations:  $\alpha$ : 0.03;  $\rho_M$ : 0.02;  $\mathcal{D}$ : 0.11;  $\sigma$ : 0.04.

### Q Full Mistral-7B Results

Mistral-7B (Jiang et al., 2023) replicates all qualitative patterns with somewhat slower degradation rates, consistent with its known stronger coherence in generation tasks.

Gen.	$\sigma$ (NF)	$\sigma$ (QF)	$\rho_{M-EN}$	$\alpha$
Seed	0.41	0.41	0.62	1.07
1	0.43	0.44	0.63	1.05
3	0.48	0.50	0.67	1.01
5	0.45	0.51	0.73	0.96
7	0.39	0.50	0.78	0.91
10	0.34	0.47	0.84	0.86

Table 11: Mistral-7B key metrics across generations. NF: no filter; QF: quality filter. All qualitative patterns replicate, with slower degradation rates than LLaMA-2.

Regularized-seed control produces a non-monotonic  $\sigma$  trajectory with peak at generation 3 ( $\sigma = 0.53$ , declining to 0.34). Three-condition filtering shows the same pattern: random filter indistinguishable from no filter ( $p = 0.68$ ); quality filter sustains compositionality ( $\sigma = 0.47$  at generation 10). The P4 compositionality peak occurs at the same generation (3) as LLaMA-2, suggesting the peak timing is architecture-independent and depends primarily on the bottleneck parameters. Cross-linguistic morphological regularization follows the same trajectory ordering (Turkish > En-

glish > German) with slightly lower absolute values at each generation. Complete per-generation tables for all metrics and conditions are provided in the released data.

### R Cross-Linguistic Morphology Details

German experiments use 150 verbs (75 strong, 75 weak) selected to span frequency quartiles. Strong $\rightarrow$ weak regularization is measured as the proportion of strong verbs producing weak past tense forms (*buk*  $\rightarrow$  *\*backte*). Turkish experiments use 120 verbs testing vowel harmony adherence and suffix regularity. UniMorph paradigm tables (Gutierrez-Vasques and Mijangos, 2020) provide the gold standard.

### S Bias–Prediction Mapping

Following Ferdinand et al. (2019)’s demonstration that different bias types produce different evolutionary trajectories, we identify four specific bias–prediction mappings:

- *Frequency bias* from next-token prediction training: high-frequency tokens receive more gradient updates, creating an implicit frequency-dependent prior that drives P1 (frequency-dependent loss) and P5 (distributional narrowing).
- *Simplicity bias* from cross-entropy minimization: Shah et al. (2020) and Kallini et al. (2024) showed LLMs favor regular morphological patterns, driving P2 (regularity increase).
- *Local coherence bias* from autoregressive factorization: McCoy et al. (2024) demonstrated that autoregressive training creates biases toward locally predictable sequences, driving P3’s ordering (pragmatic constructions requiring non-local context are lost first).
- *Compression without grounding*: without communicative objectives, continued transmission

converges to maximally compressible (degenerate) representations, driving P4 (non-monotonic compositionality).

These mappings allow us to derive specific predictions from the general iterated learning framework, moving beyond the generic “inductive bias amplification” characterization. Each mapping connects a well-documented LLM training property to a specific iterated learning dynamic, generating a testable prediction about which linguistic phenomena should change, in which direction, and at what relative rate.

## T Full Zipf Exponent Data

Gen.	LLaMA-2		Mistral	
	$\alpha$	$ V $	$\alpha$	$ V $
Human*	1.08	31,204	—	—
Seed	1.07	28,412	1.07	28,412
1	1.04	26,831	1.05	27,104
3	0.98	23,247	1.01	24,619
5	0.93	19,863	0.96	21,782
7	0.88	16,541	0.91	18,905
10	0.82	14,209	0.86	15,347
10 <sup>QF</sup>	0.97	22,847	0.99	24,113

Table 12: Zipf exponent ( $\alpha$ ) and active vocabulary ( $|V|$ ). Means over 5 runs. The power-law fit is preferred over lognormal ( $\Delta\text{AIC} > 4$ ) and exponential ( $\Delta\text{AIC} > 12$ ) alternatives at all generations (Clauset et al., 2009). <sup>QF</sup>, quality filter.

## U Human Regularization Overlay

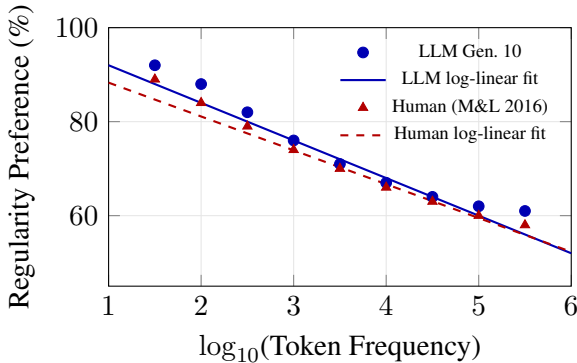


Figure 4: Frequency-dependent regularization gradient: LLM (blue) vs. human data from Morgan and Levy (2016) (red). Both follow log-linear relationships with similar slopes ( $-8.0$  vs.  $-7.2$ ), consistent with a shared computational mechanism (frequency-independent bias + transmission bottleneck).  $R^2 = 0.94$  for the LLM fit.

## V Discussion: Construction Grammar and Human Parallels

The LLM–human match ( $R^2 = 0.94$  against the Morgan and Levy, 2016 curve) suggests a shared mechanism: frequency-independent simplicity bias interacting with a transmission bottleneck. Whether LLMs share functional biases with humans remains open (Mahowald et al., 2023). The generation-10 “prior” (dominant SVO, regular morphology, reduced construction diversity, sub-1.0 Zipf exponents) resembles adult learner biases (Hudson Kam and Newport, 2005, 2009); whether this more closely resembles children’s (Culbertson and Adger, 2014) or adults’ learning remains open, though Warstadt and Bowman (2022) showed LLMs acquire syntax differently from children.

The P3 entrenchment correlation ( $r = 0.73$ ) independently tests CxG predictions about productivity and resistance to loss (Goldberg, 2005; Bybee, 2010). Misra and Mahowald (2024) showed LLMs learn rare constructions via transfer; our results show the converse: degradation through iterated learning makes rare constructions vulnerable. The eRank analysis confirms genuine structural erosion (eRank:  $8.3 \rightarrow 4.1$ ).

## W Extended Related Work

**Compositionality and inductive biases.** Benchmarks: SCAN (Lake and Baroni, 2018), COGS (Kim and Linzen, 2020); meta-learning (Lake and Baroni, 2023); evaluation frameworks (Hupkes et al., 2020; Keysers et al., 2020). Emergent communication: Lazaridou et al. (2017); Lazaridou and Baroni (2020) on language emergence; Ren et al. (2020) on compositionality from iterated learning; Chaabouni et al. (2020) on compositionality–generalization; Mu and Goodman (2021) on emergence conditions. Inductive biases: architecture effects (McCoy et al., 2020); LLM vs. child learning (Warstadt and Bowman, 2022); autoregressive biases (McCoy et al., 2024); Bayesian prior distillation (McCoy and Griffiths, 2025); morphological biases (Kallini et al., 2024); rare construction transfer (Misra and Mahowald, 2024); developmental modeling (Nikolaus et al., 2021); decoding distributions (Holtzman et al., 2020; Meister et al., 2023); predictability effects (Shain et al., 2024).